Analysis of the Calendering of Compressible Fluids

TAI-SHUNG CHUNG, *Celanese Research Company, Summit, New Jersey 07901*

Synopsis

Assuming that the compressible behavior of polymeric melt obeys the Spencer–Gilmore equation of state, the effect of melt compressibility on calendering process has been investigated. The compressible model is distinctly different from the incompressible model in three ways. (1) It has substantially lower maximum pressure, (2) the location having maximum pressure moves closer to the nip region; (3) the contact point shifts closer to the nip region.

INTRODUCTION

Calendering is one of the oldest known polymer processing techniques for producing a sheet or film of uniform thickness. The fundamental analysis of the fluid behavior in calendering was developed by Gaskell[1] and McKelvey[2] for Newtonian and power law fluids. The analysis was extended by Brazinsky et al.[3] and Kiparissides and Vlachopoulos[4], Alston and Astill[5] studied hyperbolic tangent viscosity model fluids. Chung[6] investigated Bingham plastic fluids. The nonisothermal case was solved by Dobbels and Mewis[7] and Kiparissides and Vlachopoulos.[8] Ehrmann et al.[9] developed a theoretical analysis of calendering with unequal-sized rollers. Recently, Vlachopoulos and Hrymak[10] proposed a slip model which gave improved correlation between the calculated and the measured pressure distribution.

Nearly all analyses published in the literature utilize the simplifying assumption of incompressible fluid behavior. Due to the tremendous pressure which develops in the region between the rolls, the compressibility of the molten polymer becomes significant. Thus, it is essential to examine the consequences of including compressible fluid behavior on this pressure field as a function of the operating variables in the calendering process. Therefore, the objective of this short note is to investigate the relationship between the fluid physical properties and the operational variables.

MATHEMATICAL APPROACH

The governing equations for the conservation of mass and momentum in calendering have been developed elsewhere[2–4,11,12] using the lubrication approximation.[13] For the rectangular coordinate system of Figure 1 they are

$$Q = 2\int_0^h \rho u \, dy \tag{1}$$

$$\frac{\partial P}{\partial x} = \frac{\partial}{y}\tau_{xy} \tag{2}$$

Journal of Applied Polymer Science, Vol. 28, 2119–2124 (1983)
 CCC 0021-8995/83/062119-06$01.60

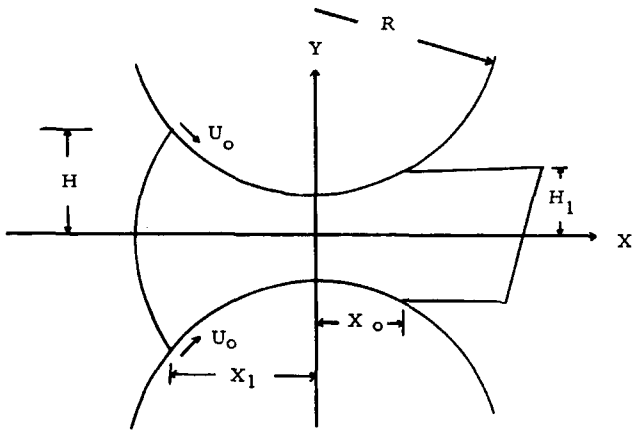

Fig. 1. Notations for the flow analysis in calendering.

Melt density follows the Spencer–Gilmore equation of state[14]

$$(P + W)(1/\rho - V_0) = R_c T \tag{3}$$

and shear stress is considered to obey the power law model

$$\tau_{xy} = m \exp\left(\frac{E}{R'T}\right)\left(\frac{\partial u}{\partial y}\right)^n \tag{4}$$

Here the effect of pressure on the melt viscosity is neglected. This effect might become important if the process pressure is extremely high.[11] For symmetric calendering, the pressure gradient can be easily obtained by solving the above equations with the boundary condition $U(h) = U_0$ and by assuming the sheet comes off the roll with the same speed U_0:

$$\frac{dp^*}{dx^*} = -\left(\frac{2n+1}{n}\right)^n \sqrt{\frac{2R}{H_0}} \frac{(\lambda^2 - x^{*2})|\lambda^2 - x^{*2}|^{n-1}}{(1 + x^{*2})^{2n+1}} \tag{5}$$

where the dimensionless variables P^*, x^*, and λ are defined as

$$P^* = \frac{P}{m}\left(\frac{H_0}{U_0}\right)^n \exp\left(\frac{-E}{R'T}\right) \tag{6}$$

TABLE I
Material Properties and Molding Conditions

Material	Polyethylene	Polystyrene
n	0.594	0.368
E/R' (°K)	2300	5910
m (P·s^{n-1})	126.9	0.5
W (psi)	47600	27000
V_0 (cc/g)	0.875	0.822
R_c (psi·cc/g·°K)	43	11.6
T (°K)	420	450
R (cm)	10	10
U_0 (cm/s)	30	30

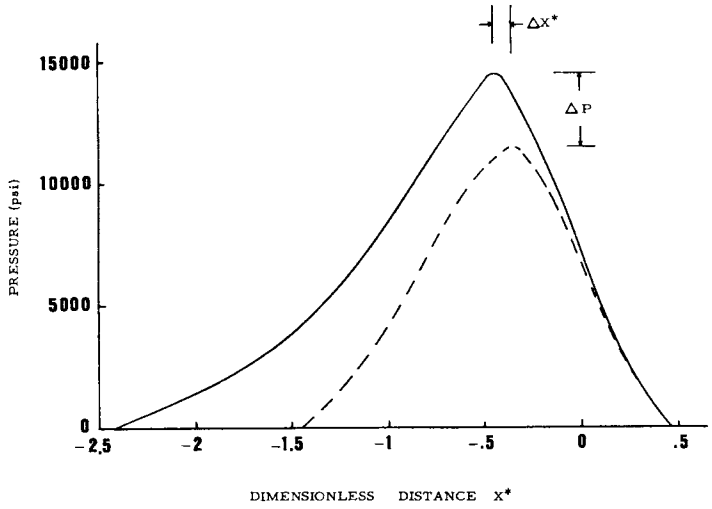

Fig. 2. Typical pressure profiles for polyethylene: (- - -) compressible model; (——) incompressible model; $\lambda_0 = 0.45$.

$$x^* = \frac{x}{\sqrt{2RH_0}} \tag{7}$$

and

$$\lambda^2 = \frac{Q}{2U_0H_0\rho} - 1 \tag{8}$$

Equation (5) is similar to that of the incompressible, non-Newtonian fluid system except that λ is no longer a constant in current studies. The pressure can be obtained by using a fourth-order Runge–Kutta integration method with the

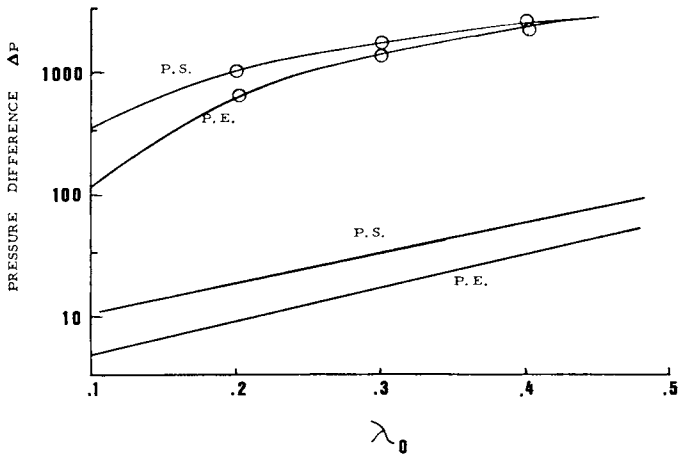

Fig. 3. Pressure difference ΔP as a function of λ_0: (——) $H_0 = 0.01$ cm; (—o—) $H_0 = 0.001$ cm.

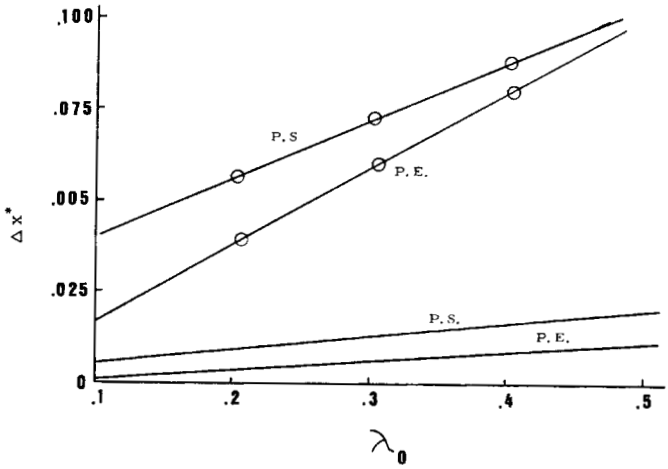

Fig. 4. Shift Δx^* as a function of λ_0: (—) $H_0 = 0.01$ cm; (—o—) $H_0 = 0.001$ cm.

following boundary condition:

$$\text{at } x = x_0, \quad P = 0, \quad U = U_0 \tag{9}$$

This boundary condition implies that at $x = x_0$

$$\lambda^2 = \lambda_0^2 = H_1/H_0 - 1 \tag{10}$$

and

$$X_0 = \lambda_0(2H_0R)^{1/2} \tag{11}$$

These results also apply to incompressible non-Newtonian fluids.

RESULTS AND DISCUSSION

Two different polymeric resins are used in calculations. Their rheological properties and thermal behavior are given in Table I.[14,15] Polystyrene generally

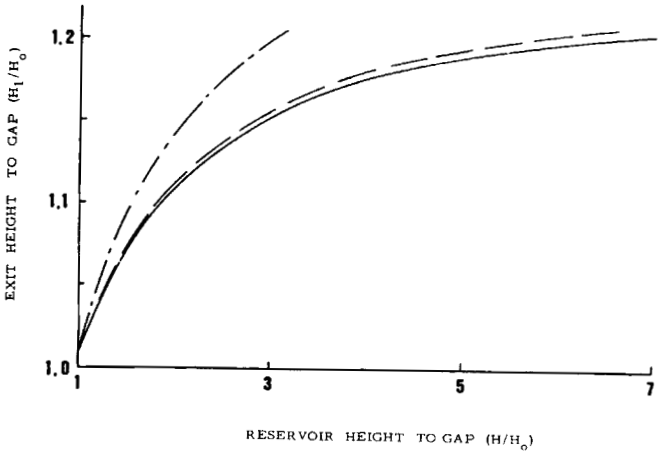

Fig. 5. Exit height (H_1/H_0) as a function of upstream reservoir thickness (H/H_0) for polyethylene: (—) incompressible model; (- - -) compressible model with $H_0 = 0.01$ cm; (-·-) with $H_0 = 0.001$ cm.

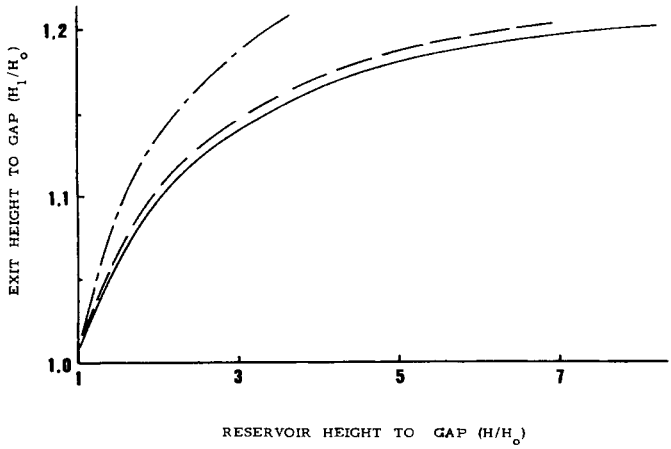

Fig. 6. Exit height (H_1/H_0) as a function of upstream reservoir thickness (H/H_0) for polystyrene: (——) incompressible model; (- - -) compressible model with H_0 = 0.01 cm; (-·-) with H_0 = 0.001 cm.

has higher melt viscosity than polyethylene, while it is less compressible than polyethylene at very high pressure. Typical pressure profiles for polyethylene compressible and incompressible models are shown in Figure 2. The compressible model has three distinct differences from the incompressible case: (1) It has substantially lower maximum pressure, (2) the location having maximum pressure moves closer to the nip region, and (3) the contact point X_1 shifts closer to the nip region.

Figures 3 and 4 give the amount of pressure difference ΔP and location movement ΔX^*, respectively. In general, polystyrene has a higher value of ΔP and ΔX^* than polyethylene when the gap between the rolls are big. However, this phenomenon tends to reverse when the gap is reduced. In other words, the pressure developed between the rolls is low if the gap is large. Polystyrene has a higher viscosity so that it develops a much larger pressure field than polyethylene. Therefore, the effect of polystyrene compressible behavior is more pronounced than that of polyethylene. However, an extremely large pressure develops in the nip region when the gap is small and melt density deviates from the incompressible case. The greater the polymer compressibility, the larger the difference in ΔP and ΔX^*.

In Figures 5 and 6, H_1/H_0 (exit height to gap height) is plotted against H/H_0 (reservoir height to gap height) for polyethylene and polystyrene fluids, respectively. When the ratio H/H_0 is kept constant, the calendering of both compressible fluids produces higher values of H_1/H_0 than those calculated by assuming incompressible fluids. This phenomenon is enhanced in the case of small gap calendering.

The above analysis clearly indicates that material compressibility strongly influences the operational variables and final products.

In addition, in agreement with previous experimental work on PVC,[10] the reduction in the magnitude of maximum pressure P and the movement of the contact point to the nip region, ΔX^*, have been observed. Perhaps due to experimental difficulty and inaccuracy, the shift of the location having maximum pressure has not been reported. Vlachopoulos and Hrymak[10] proposed a slip boundary condition in order to explain this observed difference between the

predicted and the measured values. However, the present work suggests that these differences may also be partly due to the neglect of the effect of polymer compressible behavior.

APPENDIX: NOMENCLATURE

E	flow activation energy
h	$H_0 (1 + X^2/2H_0R)$, circumference of roll near the nip region
H	reservoir height defined in Figure 1
H_0	one-half of minimum gap width
H_1	exit height defined in Figure 1
m	constant defined in eq. (4)
n	power law index
P	pressure
Q	mass flow rate
R	radius of roll
R'	gas constant
R_c	constant in eq. (3)
T	temperature
U	velocity
U_0	roll speed
V_0	constant in eq. (3)
W	constant in eq. (3)
X_1	contact point
X_0	leave-off point
ρ	density
τ	shear stress

References

1. R. E. Gaskell, *J. Appl. Mech.*, **17,** 334 (1950).
2. J. M. McKelvey, *Polymer Processing*, Wiley, New York, 1962, Chap. 9.
3. I. Brazinsky, H. F. Cosway, C. F. Valle, Jr., R. Jones, R. Clark, and V. Story, *J. Appl. Polym. Sci.*, **14,** 2771 (1970).
4. C. Kiparissides and J. Vlachopoulos, *Polym. Eng. Sci.*, **16,** 719 (1976).
5. W. W. Alston and K. N. Astill, *J. Appl. Polym. Sci.*, **17,** 3157 (1973).
6. T. S. Chung, *J. Appl. Polym. Sci.*, **25,** 967 (1980).
7. F. Dobbels and J. Mewis, *AIChE J.*, **23,** 224 (1977).
8. C. Kiparissides and J. Vlachopoulos, *Polym. Eng. Sci.*, **18,** 210 (1978).
9. G. Ehrmann, R. Takserman-Krozer, and G. S. Schenkel, *Rheol. Acta*, **16,** 240 (1977).
10. J. Vlachopoulos and A. N. Hrymak, *Polym. Eng. Sci.*, **20,** 725 (1980).
11. S. Middleman, *Fundamentals of Polymer Processing*, McGraw-Hill, New York, 1977.
12. Z. Tadmor and C. G. Gogos, *Principle of Polymer Processing*, Wiley, New York, 1979.
13. J. R. A. Pearson, *Mechanical Principles of Polymer Melt Processing*, Pergamon, New York, 1966, p. 60.
14. R. F. Westover, *Processing of Thermoplastic Materials*, E. C. Bernhardt, Ed., Reinhold, New York, 1960, Sec. 3.
15. S. Kenig, Ph.D. thesis, McGill University, Montreal, Canada, 1972.

Received September 13, 1982
Accepted January 11, 1983